

PHOTOCATHODE ACTIVITIES AT INFN LASA

L. Monaco[†], D. Sertore, INFN Milano - LASA, Segrate, Italy
 M. Krasilnikov, S.K. Mohanty¹, A. Oppelt, F. Stephan, DESY, Zeuthen, Germany
¹also at INFN Milano - LASA, Segrate, Italy

Abstract

INFN LASA photocathode lab develops and produces films that are used in high brightness photoinjectors. Besides the long-time and still on-going experience on Cs_2Te , recently we have restarted an activity on alkali-antimonide films, sensitive to visible light, exploring the possibility of their stable operation in CW machines. We report in this paper the recent results obtained both on the advancements on cesium telluride and on the characterization of alkali antimonide.

INTRODUCTION

The development and growth of photocathodes as sources of high-brightness beams is an activity that has been on-going successfully at the INFN LASA photocathode lab for decades. Activities have been mainly done on UV-sensitive photocathode films, mainly Cs_2Te , producing about 150 films, tested and used in the accelerator environments in Europe and in the US [1]. In recent years, we have restarted the activities on visible sensitive alkali-antimonide compound films done in the 90s [2] motivated by the requests of the future Continuous Wave (CW) machines. The proof-of-principle of the developed recipes would have been their test in an RF Gun environment. Therefore, in collaboration with DESY PITZ, we have designed and built a new preparation system at LASA [3], fully dedicated to visible range-sensitive photocathodes. In 2021, the first three KC_Sb films were produced at LASA and thereafter tested at PITZ [4,5]. To improve the understanding of the properties of these films, with the final aim of cathode's recipe optimization, we implemented also in this new deposition system the multi-wavelength diagnostic set-up, successfully adopted in the growing of Cs_2Te films [6].

This paper describes the on-going implementations that have been done for the UV and visible production system, with some preliminary results obtained on KC_Sb films by using the multi-wavelength diagnostic set-up.

THE TWIN PHOTOCATHODE PRODUCTION SYSTEMS AT LASA

In 2020, we started new activities with the final goal of assembly a new photocathode production system, copy of the one in operation at LASA since the 90s for Cs_2Te , to have a "twin" systems, fully compatible, but dedicated to different compounds, respectively alkali-telluride (1st system, so-called UV system) and alkali-antimonide (2nd system, so-called Green system). The duplication of the

production system was decided to limit possible cross-pollution if the two materials would have been grown in the same system, eliminating the risk of contamination once in operation in the RF guns. Moreover, the compatibility between the two systems is complete, and the same transport boxes ("suitcase") can be moved from one system to another in case particular diagnostics are required (like the QE map scans now available only on UV systems).

The new system has improved pumping system, plug temperature reading, and source holder. Since the alkali-antimonide compounds are more sensitive to vacuum quality (base pressure 10^{-11} mbar), we replaced the $400 \text{ l} \cdot \text{s}^{-1}$ ion pump with two SAES Getters NexTorr pumps to reach the required vacuum quality. The plug temperature reading was improved by a new system able to measure the plug body one; the source holder flange was completely redesigned allowing removal of evaporation sources structure during maintenance. Figure 1 shows the Photocathode production lab with the "twin" preparation systems.

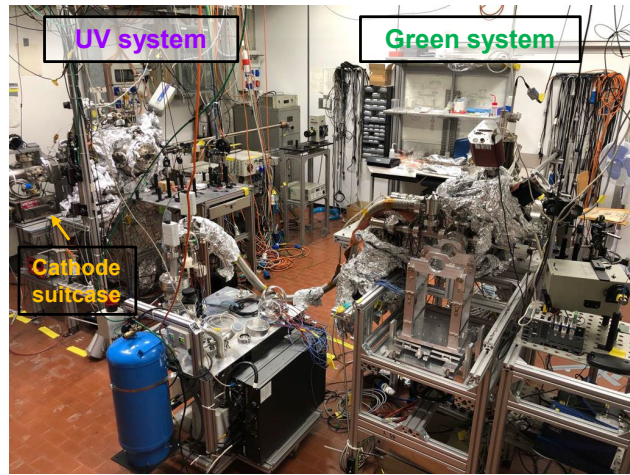


Figure 1: The "twin" systems in the photocathode production laboratory at LASA. Left: UV (Cs_2Te – alkali-telluride) system; Right: Green (alkali-antimonide) system.

The Green system is equipped with a large CF 100 viewport and two additional CF40 UV viewports, designed to directly see the front surface of the plug once in the masking allowing optical measurement at a larger angle (45°).

Furthermore, both systems are equipped with a longer longitudinal magnetic manipulator for the photocathode-carrier transfer, in preparation of the installation of the TRAnsverse Momentum Measurement (TRAMM) device for the thermal emittance measurements [7,8].

Light Sources

In the UV system, we use a Hg lamp selecting remotely wavelengths by interference filters (239 nm to 436 nm with 10 nm bandwidth). They are used during the deposition

[†] laura.monaco@mi.infn.it

process (multi-wavelength diagnostic) and for all the film characterization measurements (QE maps, spectral response, and reflectivity). In the new Green system, we use a broadband LDLS (Laser Drive Light Sources) from EQ-77 Energetiq as light sources accompanied by a set of dedicated optical filters (239 nm to 690 nm) or by a monochromator (170 nm to 1200 nm) to measure the spectral response and reflectivity during and after the production of the photocathodes. Being the photocathode grown in the Green system sensitive to visible light, we might also use He-Ne lasers in a range between 543 and 633 nm.

Acquisition System

The acquisition system for Green cathodes production is based on Labview, and it has been updated, w.r.t. the UV one, to collect the reflected power and the photocurrent at up to 8 different wavelengths. For each wavelength, total photocurrent and reflected power are recorded, with proper background signal subtraction. The sequence for the multi-wavelength diagnostic is 540- λ_s -540 nm (being 540 nm the reference λ), repeated continuously during the entire deposition process, with a ratio 540: λ_s of 1:1. The ratio in the UV production system (with 254 nm as reference λ) is typically 3:1. In addition, all other meaningful parameters like plug temperature, thickness (microbalance), pressures, etc., are recorded at each acquisition cycle. Fig. 2 and Fig. 3 show, respectively, the screenshot of the acquisition panel and the optical set-up for the multi-wavelengths diagnostic.

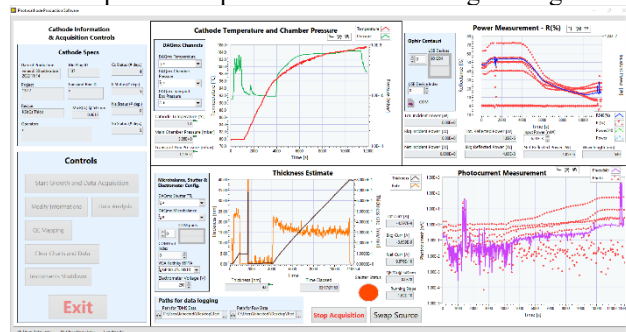


Figure 2: A screenshot of the acquisition panel during the Sb and K deposition process of photocathode 137.2.

CATHODE GROWING

Single-Wavelength Measurements

For the first batch, three KCsSb cathodes were grown in the Green preparation system, one thick and two thin (more details in ref. [4]). During this first production, the real-time photocurrent and reflectivity were monitored by a single wavelength, i.e., 543nm. Spectral responses and reflectivity's after the deposition were measured in a wide wavelength range ($\lambda_s = 254\text{nm} \div 690\text{nm}$), and they confirmed results obtained in the R&D system for sample at different thicknesses: similar spectral responses (proving that thin and thick compounds have the same composition), different reflectivity behaviour at low photon energies.

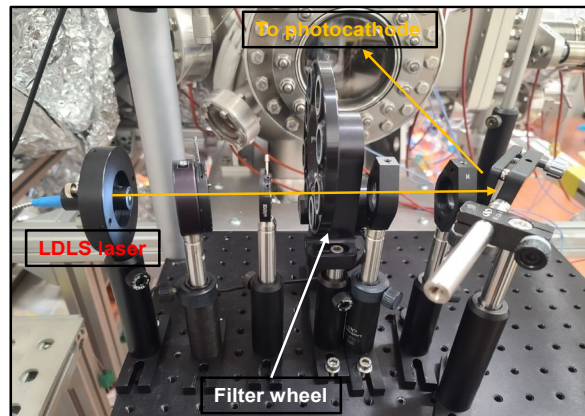


Figure 3: Multi-wavelengths measurement optical setup.

Multi-Wavelength Measurements

To better investigate real-time photoemissive and optical properties during the film deposition, with the possibility of discriminating the effect of Sb, K and Cs, we implemented the multi-wavelengths diagnostic with eight filters (254, 297, 365, 488, 515, 540, 632, 690 nm).

We deposited two photocathodes (137.2 and 137.3) with the same recipe keeping similar growing parameters (temperature, sources rate, incident power, etc.), only varying the film thickness by evaporating different Sb amounts (10 nm for 137.2, 5 nm for 137.3) to produce thick and thin films. The sequential deposition started with Sb ($T = 120^\circ\text{C}$), followed by K ($T = 150^\circ\text{C}$) until reaching the photocurrent peak and then evaporating Cs ($T = 120^\circ\text{C}$) until the completion of the compound. We have monitored the real-time photocurrent and reflectivity at 8 different wavelengths during Sb, K, and Cs of deposition. Table 1 summarizes evaporated thickness (Sb, K, Cs) and the final QE and reflectivity of both photocathodes at 540 nm.

The two above-mentioned photoemissive films have been grown on the same Mo plug. Before the second deposition, the previous film has been destroyed by a heating cycle up to 450°C and the complete removal was checked by QE and reflectivity measurements before starting with the next film evaporation.

Table 1: Evaporated Thickness, QE, And R At 540 Nm Of Cathode 137.2 (Thick) And Cathode 137.3 (Thin). Temperature: $T_{\text{sb}} = 120^\circ\text{C}$, $T_k = 150^\circ\text{C}$, $T_{\text{cs}} = 120^\circ\text{C}$.

| Cath. | Sb (nm) | K (nm) | Cs (nm) | QE* | R* |
|-------|------------|-----------|------------|-------|-------|
| 137.2 | 10.1 | 88.9 | 181.0 | 3.3 % | 22.4% |
| 137.3 | 5.3 | 53.7 | 85.1 | 3.8 % | 12.0% |

DATA ANALYSIS

The preliminary results of real-time spectral response and reflectivity data are presented in this section. Fig. 4 and Fig. 5 show the evolution of reflectivity and of QE during the Sb and K evaporation of both films, respectively.

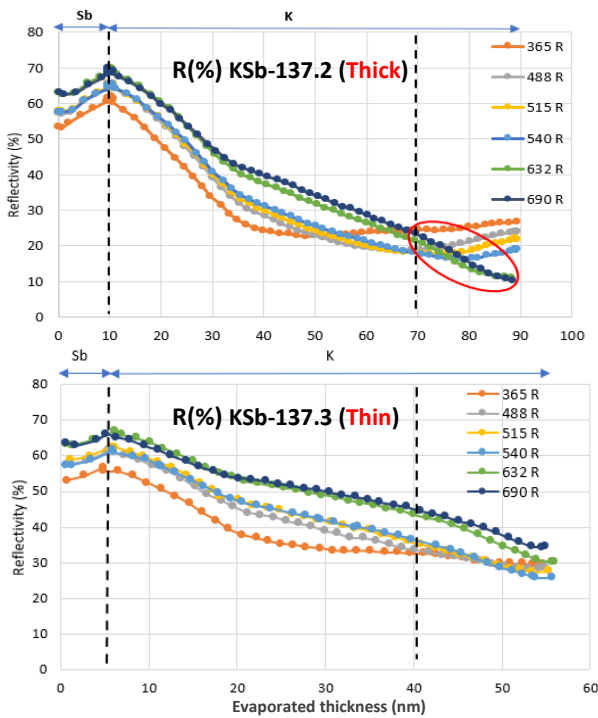


Figure 4: Reflectivity evolution at different λ s during Sb and K deposition for thick (137.2) and thin (137.3) cathodes.

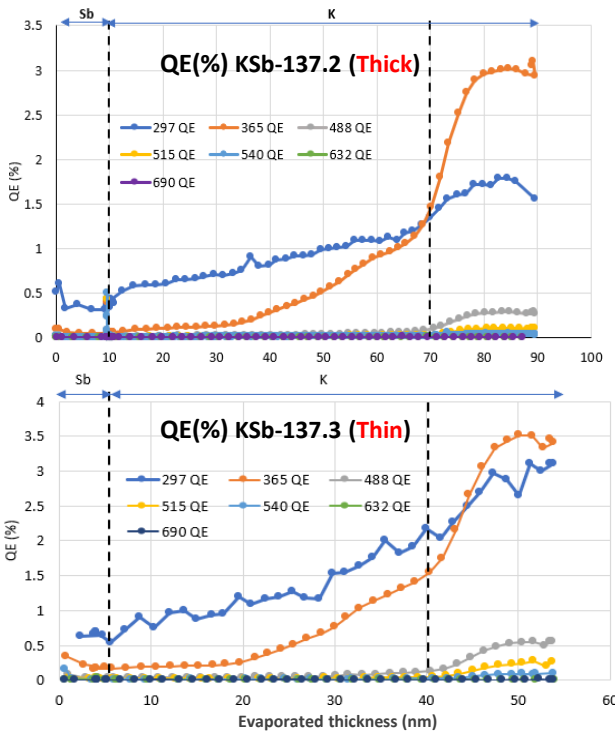


Figure 5: QE evolution at different λ s during Sb and K deposition for thick (137.2) and thin (137.3) cathodes.

During the Sb deposition both films behave similarly, with an initial reflectivity decrease, followed by an increase at all λ s. However, during K deposition, after 70 nm there is a difference in the reflectivity behaviour for cathode 137.2 (thick) between red (i.e., 632 nm, 690 nm) and

visible wavelengths (i.e., 488 nm, 515 nm, 540 nm). Differently on cathode 137.3 (thin), there is no significant difference in the reflectivity behaviour (at all the wavelengths).

If we compare real-time reflectivity with real-time QE data during the K evaporation for the cathode 137.2 (see Fig. 5), we observe that the difference in the reflectivity behaviour only appeared in correspondence of a jump (or sharp change in slope) in the QE curve. It indicates that this reflectivity behaviour may stem from the different composition or crystal modifications of the K-Sb film [9], or from the thicknesses of the K-Sb films changing, as observed for Cs₂Te [10]. The analysis is on-going, and the detailed interpretation will be published in the upcoming publication.

Fig. 6 illustrates the spectral response and reflectivity of cathodes 137.2 & 137.3 after the deposition. As can be observed in, both the thick and thin photocathodes exhibit a similar spectral response, while the reflectivity at low photon energy behaves differently. This difference in the reflectivity behaviour has previously been observed between thick and thin cathodes in our past R&D experience [5,11]. Furthermore, as it can be observed, the thick and thin cathodes exhibit a different reflectivity peak in the infrared region, i.e., 1.05 eV and 1.22 eV, respectively.

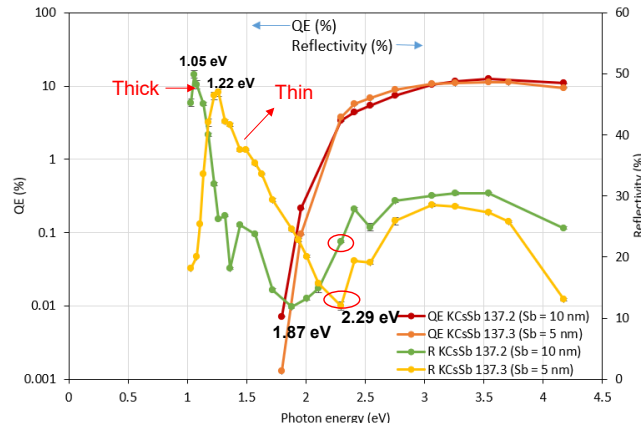


Figure 6: Spectral response and reflectivity after deposition of thick (137.2) and thin (137.3) cathodes.

CONCLUSION

Studies on UV and green films using the multi-wavelength technique are useful to better understand coatings' photoemissive and optical properties. The analysis of the real-time QE and reflectivity (at different wavelengths) are still underworking, but significant differences between thin and thick KCsSb cathodes have been here reported.

The availability of this diagnostic (with the other already available) on the two production systems at LASA is a powerful tool for a deeper study on the coating properties and for the possibility to test them in gun environment, also doing post-diagnostic after operation.

ACKNOWLEDGEMENTS

We acknowledge DESY Zeuthen for the fruitful collaboration for testing these photocathodes in the PITZ RF

guns. This work is also supported partially by the European XFEL research and development program.

REFERENCES

- [1] C. Pagani *et al.*, "LASA Cs₂Te Photocathodes: the Electron Source for XFELs", in Congress of the Department of Physics, Springer. 2017, pp 281-292. ISBN: 978-3-030-01629-6.
- [2] P. Michelato *et al.*, "R&D activity on high QE photocathodes for RF guns", in *Proc. 16th Particle Accelerator Conf. (PAC'95)*, Dallas, TX, USA, May 1995, pp. 1049-1051. doi:10.1109/PAC.1995.505125
- [3] S.K. Mohanty *et al.*, "Development of multi-alkali antimides photocathodes for high-brightness RF photoinjectors", in *Proc. 12th Int. Particle Accelerator Conf. (IPAC'21)*, Campinas, SP, Brazil, May 2021, pp. 1416-1419. doi:10.18429/JACoW-IPAC2021-TUPAB034
- [4] D. Sertore *et al.*, "R&D high QE photocathodes at INFN", in Proc. 13th Int. Particle Accelerator Conf. (IPAC'22), Bangkok, Thailand, June 2022, pp. 2633-2636. doi:10.18429/JACoW-IPAC2022-THPOPT027
- [5] S.K. Mohanty *et al.*, "Development and test results of multi-alkali antimonide photocathodes in the high gradient RF Gun at PITZ", presented at the 40th Int. Free Electron Laser Conf. (FEL'22), Trieste, Italy, Aug. 2022, paper TUP04, unpublished.
- [6] L. Monaco *et al.*, "Multi-wavelengths optical diagnostic during Cs₂Te photocathodes deposition", in Proc. 1st Int. Particle Accelerator Conf. (IPAC'10), Kyoto, Japan, May 2010, paper TUPEC006, pp. 1719-1721.
- [7] D. Sertore *et al.*, "Assembly and characterization of low-energy electron TRAnsverse Momentum Measurement device (TRAMM) at INFN LASA", in Proc. 13th Int. Particle Accelerator Conf. (IPAC'22), Bangkok, Thailand, June 2022, pp. 2630-2632. doi:10.18429/JACoW-IPAC2022-THPOPT026
- [8] D. Sertore *et al.*, "Status of a low-energy electron TRAnsverse Momentum Measurement device (TRAMM) at INFN LASA", presented at the 14th Int. Particle Accelerator Conf. (IPAC'23), Venice, Italy, May 2023, paper TUPA007, this conference.
- [9] M. Ruiz-Os'es *et al.*, "Direct observation of bi-alkali antimonide photocathodes growth via in operando x-ray diffraction studies", A.P.L. vol. 2, p. 121101, 2014. doi:10.1063/1.4902544
- [10] L. Monaco *et al.*, "Growing and characterization of Cs₂Te photocathodes with different thicknesses at INFN LASA", in *Proc. 39th Free Electron Laser Conf. (FEL'19)*, Hamburg, Germany, August 2019, pp. 297-2632. doi:10.18429/JACoW-FEL2019-WEA04
- [11] S.K. Mohanty *et al.*, "Development of a multialkali antimonide photocathode at INFN LASA", in *Proc. 39th Free Electron Laser Conf. (FEL'19)*, Hamburg, Germany, August 2019, pp. 448-451. doi:10.18429/JACoW-FEL2019-WEPO53